Title

Afadin orients cell division to position the tubule lumen in developing renal tubules

Journal

Development, 144(19)

ISSN

0950-1991

Authors

Gao, Lei
Yang, Zhufeng
Hiremath, Chitkale
et al.

Publication Date

2017-10-01

DOI

10.1242/dev.148908

Peer reviewed

Elsevier Editorial System(tm) for Cellular Signalling

Manuscript Draft

Manuscript Number:

Title: Fibroblast-derived HGF drives acinar lung cancer cell polarization through integrin-dependent RhoA-ROCK1 inhibition.

Article Type: Full Length Article

Keywords: Epithelia; Cell Polarity; HGF; MET; RhoA; ROCK1

Corresponding Author: Dr. David Bryant,

Corresponding Author's Institution:

First Author: Anirban Datta

Order of Authors: Anirban Datta; Emma Sandilands; Keith Mostov; David Bryant

Abstract: Formation of lumens in epithelial tissues requires apical-basal polarization of cells, and the co-ordination of this individual polarity collectively around a contiguous lumen. Signals from the Extracellular Matrix (ECM) instruct epithelia as to the orientation of where basal, and thus consequently apical, surfaces should be formed. We report that this pathway is normally absent in Calu-3 human lung adenocarcinoma cells in 3-Dimensional culture, but that paracrine signals from MRC5 lung fibroblasts can induce correct orientation of polarity and acinar morphogenesis. We identify HGF, acting through the c-Met receptor, as the key polarity-inducing morphogen, which acts to activate B□1-integrin-dependent adhesion. HGF and ECM-derived integrin signals co-operate via a c-Src-dependent inhibition of the RhoA-ROCK signalling pathway via p190A RhoGAP. This occurred via controlling localization of these signalling pathways to the ECM-abutting surface of cells in 3-dimensional culture. Thus, stromal derived signals can influence morphogenesis in epithelial cells by controlling activation and localization of cell polarity pathways.

Suggested Reviewers: Gerard Apodaca
Department of Medicine Renal-Electrolyte Division & Department of Cell Biology, University of Pittsburgh
gla6@pitt.edu
An expert in epithelial cell biology

James Goldenring
Vanderbilt University
jim.goldenring@Vanderbilt.Edu
An expert in epithelial biology

Charles Campbell
Centre for Cancer Research and Cell Biology, Queen's University Belfast
f.c.campbell@qub.ac.uk

Fernando Martin-Belmonte

Centro de Biología Molecular Severo Ochoa (CBMSO)
fmartin@cbm.csic.es
An expert in epithelial 3D biology.

Denise Marciano
UT Southwestern
denise.marciano@utsouthwestern.edu

Joshua Lipschutz
Medical University of South Carolina
lipschut@musc.edu
An expert in 3D biology

Opposed Reviewers: Charles Streuli

Mina Bissell

Andrew Ewald

University of Glasgow | Institute of Cancer Sciences

Thursday, 3 August 17

Editor, Cellular Signaling

Please find accompanying this letter a manuscript by Datta, Sandilands, Mostov and Bryant titled, "*Fibroblast-derived HGF drives acinar lung cancer cell polarization through integrin-dependent RhoA-ROCK1 inhibition*".

Formation of an epithelial lumen lined by polarised epithelial cells is an obligatory step for metazoan life. This requires not only the apical-basal polarization of cells, but the co-ordination of each cell's polarity collectively around a single central lumen. While much is known about the signaling pathways that control apical-basal polarity, our understanding of how cells know to place their apical-basal polarity in the correct orientation is much more rudimentary. We previously reported (Yu, *EMBO Rep*, 2008; Bryant, *Dev Cell*, 2014) that epithelial cells require cues from the Extracellular Matrix to correctly orient this polarity. Such cues are transduced by integrin molecules, ultimately feeding in to regulation of the RhoA signaling pathway to control where an apical surface is formed.

Here, we describe that cross-talk between lung fibroblast and lung cancer cells controls the 3-Dimensional morphogenesis of epithelial cells. We elucidate a molecular signaling pathway that controls switching between two polarised states in 3D epithelia: inverted or luminally oriented. In 3D Calu-3 lung cancer cells, the RhoA signaling pathway controlling polarity is inappropriately active and blocks the formation of polarised 3D acini around a central lumen. Strikingly, we find roles for both EGF and HGF derived from fibroblasts in controlling polarization: EGF controls growth of the epithelial cells, while HGF stimulated the correct orientation of acinar polarity.

We reveal that Calu-3 cells at steady state have poor activation of β1-integrin signaling pathways, and are thus partially defective in polarization. Fibroblast-derived HGF stimulates correct polarity orientation in Calu-3 by stimulating c-Src-dependent localization of β1-integrins, and basolateral recruitment of the Rho GAP protein, p190A RhoGAP. This in turn inactivates RhoA and its effector protein ROCK1, allowing 3D acini to form around a single central lumen. **We therefore reveal that cross-talk between fibroblasts and epithelial cells can control the polarization state of epithelia.** Though commonly adjacent *in vivo*, the effect of fibroblasts on regulating epithelial polarity is poorly understood, and thus we believe that these results are of exceptional interest to a broad range of Cellular Signaling readers in cell biology, development, and cancer.

Yours sincerely,

Dr. David M. Bryant
College of Medical, Veterinary & Life Sciences
CRUK Beatson Institute & Institute of Cancer Sciences
Garscube Estate, Switchback Road, Bearsden, Glasgow G61 1QH
Tel: 0141 330 8597
Email: david.bryant@glasgow.ac.uk
http://tinyurl.com/davidbryantlab

University of Glasgow | Institute of Cancer Sciences

Dr. David M. Bryant
College of Medical, Veterinary & Life Sciences
CRUK Beatson Institute & Institute of Cancer Sciences
Garscube Estate, Switchback Road, Bearsden, Glasgow G61 1QH
Tel: 0141 330 8597
Email: david.bryant@glasgow.ac.uk
http://tinyurl.com/davidbryantlab

Highlights

- Lung fibroblast-derived EGF and HGF induces acinar morphogenesis of Calu-3 cells.
- HGF activates β1-integrin-dependent adhesion, whilst EGF stimulates proliferation.
- HGF and β1-integrin converge to inhibit RhoA-ROCK1 signalling thereby regulating polarity orientation.

Abstract

Formation of lumens in epithelial tissues requires apical-basal polarization of cells, and the co-ordination of this individual polarity collectively around a contiguous lumen. Signals from the *E*xtra*c*ellular *M*atrix (ECM) instruct epithelia as to the orientation of where basal, and thus consequently apical, surfaces should be formed. We report that this pathway is normally absent in Calu-3 human lung adenocarcinoma cells in 3-Dimensional culture, but that paracrine signals from MRC5 lung fibroblasts can induce correct orientation of polarity and acinar morphogenesis. We identify HGF, acting through the c-Met receptor, as the key polarity-inducing morphogen, which acts to activate β1-integrin-dependent adhesion. HGF and ECM-derived integrin signals co-operate via a c-Src-dependent inhibition of the RhoA-ROCK signalling pathway via p190A RhoGAP. This occurred via controlling localization of these signalling pathways to the ECM-abutting surface of cells in 3-dimensional culture. Thus, stromal derived signals can influence morphogenesis in epithelial cells by controlling activation and localization of cell polarity pathways.

Fibroblast-derived HGF drives acinar lung cancer cell polarization through integrin-dependent RhoA-ROCK1 inhibition.

Anirban Datta[1,2,3], Emma Sandilands[4], Keith E. Mostov[1,2], David M. Bryant[4,5,6]

Dept. of [1]Anatomy, [2]Biochemistry and Biophysics, University of California San Francisco, CA 94158-2140, USA.
[3]Current address: Verseon Corporation, Fremont, CA 94538, USA.
[4]Institute of Cancer Sciences, and [5]The CRUK Beatson Institute, University of Glasgow, Glasgow G61 1BD, United Kingdom.

[6]Correspondence: DMB (david.bryant@glasgow.ac.uk)

Abstract

Formation of lumens in epithelial tissues requires apical-basal polarization of cells, and the co-ordination of this individual polarity collectively around a contiguous lumen. Signals from the *E*xtra*c*ellular *M*atrix (ECM) instruct epithelia as to the orientation of where basal, and thus consequently apical, surfaces should be formed. We report that this pathway is normally absent in Calu-3 human lung adenocarcinoma cells in 3-Dimensional culture, but that paracrine signals from MRC5 lung fibroblasts can induce correct orientation of polarity and acinar morphogenesis. We identify HGF, acting through the c-Met receptor, as the key polarity-inducing morphogen, which acts to activate β1-integrin-dependent adhesion. HGF and ECM-derived integrin signals co-operate via a c-Src-dependent inhibition of the RhoA-ROCK signalling pathway via p190A RhoGAP. This occurred via controlling localization of these signalling pathways to the ECM-abutting surface of cells in 3-dimensional culture. Thus, stromal derived signals can influence morphogenesis in epithelial cells by controlling activation and localization of cell polarity pathways.

Keywords

Epithelia; Cell Polarity; HGF; MET; RhoA; ROCK1

1. Introduction

A simple epithelial monolayer consists of apical-basal polarized epithelial cells, which are the basic building block of acini in organs [1]. Epithelial cells possess functionally specialized basolateral and apical cell surfaces. The basolateral domain, although contiguous, is often described as two independent domains due to their distinct functional properties: the basal surface contacts the underlying *e*xtra*c*ellular *m*atrix (ECM) and the lateral surface allows adherence to neighbouring cells, while also providing a paracellular diffusion barrier [2]. In contrast, the apical surface provides the lining of the lumen of epithelial tissues, possessing the distinct characteristic of non-adherence to neighbours or the ECM. Such polarity on an individual level must be collectively coordinated between neighbouring cells to form the lumen and thus a biological tube.

While the mechanisms of how apical-basal polarity is formed has been extensively investigated [1, 2] how such polarity is oriented has until recently been largely neglected [3, 4]. Traditional culture methods for epithelial cells involves growth of cells to become apical-basal polarized monolayers on rigid substrata such as glass, plastic, or semi-permeable membrane filters. In these systems, the stiff culture vessel provides an immediate and strong cue to where basal membranes should form [5]. In contrast, in 3-Dimensional (3D) culture where single epithelial cells are embedded in ECM gels, such as Matrigel or collagen, cells are surrounded by ECM. In such isotropic conditions, mechanisms must exist to orient apical-basal polarity formation such that the basal surface faces the ECM and the apical surface lines the cavity of ‘free space’.

We have described that temporospatial control of the RhoA signalling pathway is essential for the correct orientation of apical-basal polarity [6, 7]. In the MDCK cyst model, upon embedding isolated MDCK cells into Matrigel gels, single cells divide to form a cell doublet that has initially inverted polarity, i.e. apical surfaces erroneously facing the ECM. Detection of the ECM by β1-integrin-dependent adhesion results in phosphorylation of the RhoA-inhibitor GAP p190A RhoGAP [6]. P190A leads to inactivation of RhoA-ROCK1 signalling, at the ECM abutting surface, allowing endocytosis of apical proteins from the ECM-abutting

periphery and transcytosis to the centre of the cell doublet to form a lumen. This results in the correct orientation of apical-basal polarity between cells in 3D culture.

An open question from our and others' previous studies is how generalizable signalling pathways identified to regulate polarity orientation in one cell type are to other epithelia? In addition, are these pathways defective in epithelial cancer cells? In the current work, we show that the previously identified pathway for correct polarity orientation is inactive in Calu-3 human lung adenocarcinoma cells grown in 3D at steady state. Fibroblast-derived signals, particularly HGF, can correct aberrant polarity orientation in 3D by controlling the localization of polarity pathways to the ECM-abutting surface. This suggests that future studies into modulation of this pathway may be important for understanding polarity changes in cancer.

2. Materials and Methods

2.1.2-Dimensional and 3-Dimensional culture.

3D culture of Calu-3 was performed using adaptations of that described for MDCK [6]. Calu-3 (ATCC HTB-55) were grown in Eagle's Minimum Essential Medium supplemented with 10% fetal bovine serum (FBS; Gibco). For plating in 3D, single cell suspensions were made (2×10^4 cells ml^{-1}) in growth medium supplemented with 2% Matrigel (BD Biosciences). Cell:medium:Matrigel mixture was plated onto Matrigel-pre-coated (15µl of net Matrigel) 8-well coverglass chambers (Nunc, LabTek-II). At appropriate times paraformaldehyde (PFA) was used to fix cells. For induction of acinar morphogenesis, cells were treated at day 4 with modifiers and fixed at day 9. Modifiers included MRC5 lung-derived fibroblast-conditioned medium (FCM), HGF blocking antibody (0.1 µg/mL; R&D Systems, 24612), SU11274 (10 µM; Tocris), EGF (10 ng/ml, PeproTech, AF-100-15), HGF (10 ng/ml, gift from Genentech), Iressa (1 µM; SigmaAldrich, SML1657), AIIB2 (1:200; a gift of C. Damsky, UCSF), TS2/16 (1:100; a gift of C. Damsky, UCSF), PP2 (5 µM, Sigma-Aldrich, P0042), Y-27632 (10 µM, Calbiochem, 688002), LY-294002 (10 µM; Calbiochem, 440204), Akt Inhibitor II (10 µM; Calbiochem, 124008), rapamycin (20nM; Calbiochem, 553211), or UO126 (10 µM; Cell Signaling Technology, 9903). MRC5 (ATCC) were cultured in Eagle's Minimum Essential Medium supplemented with 10% fetal bovine serum (FBS; Gibco). For production of condition medium MRC5 were grown as previously described [8] to confluence in Eagle's Minimum

Essential Medium supplemented with 10% fetal bovine serum, 100 U/ml penicillin, 100 mg/ml streptomycin, in tissue culture flasks (T75; Corning). Fresh medium was replaced (30 ml) before culture for 3 days. Fibroblast conditioned medium was centrifuged at 3,500 x g to remove cell debris, and frozen at -20°C.

2.2. Antibodies and immunolabelling.

Calu-3 in 3D culture were stained essentially as described for MDCK cysts [9]. Primary antibodies utilized were: Ki-67 (Epitomics, 2642-1), Cleaved Caspase 3 (Cell Signaling Technology, 9661L), JAM-A (BD Biosciences, 612120), Muc1 (Epitomics, 2900-1), GM130 (BD Biosciences, C65120), β-catenin (Santa Cruz, sc-7199), NHERF1 (Abcam, ab3452), Ezrin (BD Biosciences, 610603), Cleaved Caspase 8 (Cell Signaling Technology, 9496), β1-integrin (BD Biosciences, 610467), pY416-c-Src (Cell Signaling Technology, 6943P), pY1105-p190 (Abcam, ab55339). Alexa fluorophore-conjugated secondary antibodies (1:250) or Phalloidin (1:200) (both Invitrogen) and Hoechst to label nuclei (10 µg/ml), were utilized. Imaging was performed on a Zeiss 510 Confocal Microscope, using a 63x oil immersion lens. Image processing was performed using ImageJ. Images shown are representative of 3 separate experiments.

2.3. Immunoblotting.

Protein blotting was performed as described [6]. To solubilize cells, cultures were washed twice in ice-cold PBC, before addition of ice-cold extraction buffer [50 mM Tris-HCl pH 7.4, 150 mM NaCl, 0.5 mM $MgCl_2$, 0.2 mM EGTA, and 1% Triton X-100 plus 50 mM NaF, 1 mM Na_3VO_4 and complete protease inhibitor cocktail tablet (Roche, Mannheim, Germany)]. Lysates were extracted at 4°C for 25 min. For 3D cultures a 27½ -gauge needle was used for assisting extraction from ECM. To remove debris, centrifugation at 14,000 x *g* at 4°C for 10 min was performed. Samples were separated using SDS-PAGE, and were transferred to PVDF membranes. Western analysis was performed using either chemiluminescence (SuperSignal Chemiluminescence Kit; Pierce, Rockford, IL) or infrared fluorescent secondary antibodies and quantitative detection (Odyssey CLx, Li-COR Biosciences). A BCA Protein Assay Reagent kit (Pierce) was used to determine protein concentration. Transfer and protein loading were monitored by staining 0.1% Coomassie Brilliant Blue. For Human Phospho-kinase array experiments (R&D

Systems, ARY003), lysates from 3D culture were processed according to manufacturer instructions. Antibodies for WB were: GAPDH (Millipore, MAB374), pY416-c-Src (Cell Signaling Technology, 6943P), Total c-Src (Cell Signaling Technology, 2102P), pY1105-p190 (Abcam, ab55339), P190A (BD Biosciences, 610149), RhoA (Santa Cruz, sc-418), Phospho-Myosin Light Chain 2 (Ser19; Cell Signaling Technology, 3671L), ROCK1 (Santa Cruz, sc-17794), ROCK2 (Santa Cruz Biotechnology, sc-100425), pY845-EGFR (Abcam, ab97613), EGFR (Cell Signaling Technology, 2232), ppERK1/2 (Cell Signaling Technology, 9107).

2.4. RNAi, virus production and transduction.

Stable depletion of proteins was performed using pLKO.1-puro lentiviral shRNA vectors, obtained from the TRC collection. Sequences and clone identities are as follows: shScramble (5'-CCTAAGGTTAAGTCGCCCTCG-3') [10], shc-Src_1 (TRCN0000038149, 5'-GCTCGGCTCATTGAAGACAAT-3'), shc-Src_2 (TRCN0000038150, 5'-GACAGACCTGTCCTTCAAGAA-3'), p190ARhoGAP_1 (TRCN0000022188, 5'-CGGTTGGTTCATGGGTACATT-3'), p190ARhoGAP_2 (TRCN0000022184, 5'-GCCCTTATTCTGAAACACATT-3'), shRhoA_1 (TRCN0000047710, 5'-GTACATGGAGTGTTCAGCAAA-3'), shRhoA_2 (TRCN0000047711, 5'-TGGAAAGACATGCTTGCTCAT-3'), shROCK1_1 (TRCN0000121094, 5'-CGGTTAGAACAAGAGGTAAAT-3'), shROCK1_2 (TRCN0000121095, 5'-GCATTCCAAGATGATCGTTAT-3'), shROCK2_1 (TRCN0000000978, 5'-GCACAGTTTGAGAAGCAGCTA-3'), shROCK2_2 (TRCN0000000981, 5'- CCTCAAACAGTCACAGCAGAA-3').

To produce lentiviral particles, pLKO plasmids were co-transfected with Virapower (Invitrogen) lentiviral packaging mix into packaging cells according to manufacturer instructions (297-FT, Invitrogen). At time of collection, viral supernatants were centrifuged twice at 3500 x g to remove cell debris. Cells were transduced with lentiviruses the day after plating, and were infected for 60 hours, before selection with puromycin (5 µg/ml, Life Technologies, A11138-03). Efficient depletion was verified using Western blotting. To stably express EGFR mutants, retroviral transductions were performed. pBabe-puro-EGFR L858R (Addgene plasmid # 11012) pBabe-puro-EGFR (del3) L747-E749del, A750P (Addgene plasmid # 11015) were a gift from Matthew Meyerson.

For production of retroviral supernatants, plasmids were transfected into 293-GPG packaging cells and medium was collected from days 5-7 after transfection. Cell debris were removed by centrifugation at 5,000 x g, twice. 16 h post-plating cells were transduced with viral supernatants supplemented with 10 μg ml−1 Polybrene (Millipore) for 24 h at 32 °C. Upon changing to fresh medium, cells were incubated for a further 48 h at 37 °C, before passage into puromycin (5 μg/ml).

2.5 Adhesion Assay.

To determine adhesion capability to laminin, 96 well plates were coated with 10ug/ml laminin-1 (BD, 354239) in PBS+ at 37°C for 30 min. Wells were washed with PBS to remove non-bound laminin-1 before blocking of non-coated regions with 1% BSA solution (SigmaAldrich) in PBS+ for 30 min. Isolated Calu-3 cells were seeded at 10,000 cells per well of a 96-well plate (100,000 cells/ml in 100ml per well) in adhesion buffer (HBSS, 10mM HEPES, 2mM Glucose) and incubated for 1 hour. Wells were gently washed with PBS to remove unbound cells. Adhesion to the well was determined by staining with Calcein AM (LifeTechnologies) for 5 min, and reading for fluorescence in a microplate reader.

2.6 FACS Analysis.

For quantitation of surface β1-integrin levels, cells were washed twice with PBS, trypsinised, centrifuged at 1,500 RPM then re-suspended in 500 μl of FACS buffer (PBS+0.1% heat inactivated BSA) and kept on ice. For primary antibody labelling with β1-integrin (BD Biosciences, 610467), cells were centrifuged and re-suspended in 100 μl of FACS buffer containing a 1:200 dilution of primary antibody and incubated on ice for 30 min. Cells were washed twice by sequential addition of 1 ml FACS buffer followed by centrifugation as above. Alexa488 secondary antibody (ThermoScientific) was added according to the antibody staining as above. Two rounds of washing were performed before surface integrin was measured using a FACS Aria 2 (BD).

2.7 Statistical tests.

Quantitation of 3D acinus formation was performed as adapted from MDCK cultures as previously described [9]. The percentage of acini displaying a single

central lumen was determined, and compared to control cell aggregates. Values are mean ± s.d. from three replicate experiments, with *n* ≥100 cysts per replicate. Significance was calculated using a paired, two-tailed Student's *t*-test.

3. Results and Discussion

3.1 Fibroblast-Conditioned Medium induces acinar polarization of Calu-3 in 3-Dimesional culture.

We examined the morphogenesis of a lung adenocarcinoma cell line Calu-3 in 3-Dimensional (3D) culture, which are thought to be derived from a tumour of the bronchial submucosal glands [11]. 3D culture of Calu-3 for up to 9 days in standard growth medium (Methods and Materials) failed to induce acinar morphogenesis, forming solid multicellular aggregates (Fig. 1A, B). We next examined, the influence of soluble factors secreted by an established lung stromal fibroblast cell line (MRC5) on Calu-3 3D morphogenesis. We cultured Calu-3 cells for 9 days, modifying the medium by the addition of various factors from days 4-9 (Fig. 1A). 3D culture of Calu-3 from the first day in MRC5 lung fibroblast-conditioned medium (FCM) resulted in both small aggregate formation and individual cell invasion (not shown). In contrast, changing the culture medium to FCM from day 4-9 induced striking morphogenetic rearrangements of the Calu-3 cells, resulting in lumen-containing acini (Fig. 1A-B). We thus used this 4+5 day schedule for subsequent experiments.

The first notable event in FCM-induced morphogenesis was the transition of cell aggregates from a non-spherical cluster into a sphere by day 5 (d5) (Fig. 1C). Subsequently, cells not rearranged into the acinus wall were cleared, concomitant with the appearance of a central lumen, and resulting in a cleared and expanded lumen by d9. Examination of proliferation (Ki-67) and apoptosis (cleaved caspase-3) markers in response to FCM revealed a redistribution of proliferation markers from all cells (d4) to solely the acinus wall (d9), while apoptosis could be observed in the lumen (d6-8; Fig 1C). FCM-treated acini possess luminal surface localization of the apical proteins Muc1, NHERF1 and Ezrin, apically oriented Golgi, and basolateral surface β-catenin and JAM-A (Fig. 1D). Without FCM, basolateral protein and Golgi orientation appeared randomized, while apical proteins were oriented towards the

ECM (Fig. 1D). This suggests that FCM caused a polarity reversion accompanied by formation of polarized acini.

3.2 HGF induces acinar morphogenesis whilst EGF stimulates proliferation.

We aimed to determine the morphogenetic factor(s) in FCM that induce Calu-3 acinar morphogenesis. Hepatocyte Growth Factor (HGF) is a key morphogen that MRC5 secrete to induce tubulogenesis of MDCK cysts [8, 12]. Surprisingly, signalling by HGF and its receptor, c-Met, was both necessary and sufficient to induce acinus formation by Calu-3 (Fig. 2A). HGF-induced morphogenesis mirrored that observed for FCM, converting non-apoptotic cell aggregates into polarized acini with lumens that display apoptotic remnants (Fig. 2B). HGF stimulation also caused a bi-phasic transactivation of the EGFR, resulting in strongly attenuated activation in the first 24h of stimulation, before a gradual return and then elevation of EGFR phosphorylation (Fig. S1A). In contrast to HGF, EGFR signalling was required for proliferation, rather than polarity orientation. Addition of EGF alone resulted in enlarged, though still inverted 3D structures (Fig. 2C). Inhibition of EGFR signalling in HGF-treated acini failed to block lumen formation, instead resulting in small, but still polarized structures (Fig. 2D). Expression of two different activated mutants of EGFR in addition to HGF stimulation resulted in spherical acini that became somewhat disorganized and poorly cleared the lumen, an effect which could be reversed using an EGFR inhibitor (Fig. 2E-F). The initial decrease in EGFR activation upon HGF stimulation (24h, Fig. S1A) likely facilitates apoptosis of the inner cells required to clear the lumen. These data suggest that both HGF and EGF regulate Calu-3 acinus formation, determining polarity and proliferation, respectively.

3.3 Acinar morphogenesis involves β1-integrin-dependent adhesion and c-Src kinase.

MDCK grown in 3D can form either apical-basal polarized cysts surrounding a central lumen, or can be induced to form front-rear polarized structures with inverted polarity by perturbing signalling from the ECM [9]. We examined whether HGF modulates ECM signalling in Calu-3 cells. In 2D culture conditions on plastic, Calu-3 grow as loosely adherent aggregates (Fig. 3A). Addition of HGF in 2D resulted in morphogenetic rearrangement whereby cells now flattened and spread on the plastic

substratum. We measured adhesion of freshly plated cells to the substrate, and found that in contrast to the normally low adhesive index of Calu-3, HGF induced strong adhesion of cells (Fig. 3B). This could be completely blocked by inhibition of β1-integrins, as could steady state adhesion levels. Strikingly, activating antibodies to β1-integrins alone were sufficient to induce adhesion of Calu-3, to levels above that of HGF alone, and could further enhance the effect of HGF (Fig. 3B). These data suggest that HGF may act to induce morphogenesis by activating β1-integrin signalling.

β1-integrin similarly controlled 3D morphogenesis. Inhibiting β1-integrins in 3D completely blocked the effect of HGF on acinar morphogenesis. Strikingly, activating β1-integrin alone was sufficient to induce acinar morphogenesis (Fig. 3C, D). In 3D, combined HGF treatment and β1-integrin experimental activation failed to cause acinar morphogenesis, suggesting that each treatment may maximally activate β1-integrins in this system. These data suggest that β1-integrins signalling pathway may be inactive in Calu-3 at steady state, and activation by HGF or antibodies is sufficient to restore 2D adhesion and 3D acinus formation.

We examined the mechanism of HGF-induced β1-integrin function. In 2D, HGF simulation did not alter the distribution of β1-integrins on the surface (Fig. 3E) suggesting that integrin activation, rather than localization, may be important. In 3D, β1-integrin localized to the cell cortex in an apparently unpolarised fashion. In contrast, HGF induced a rearrangement of polarity such that β1-integrin now only localized to basolateral membranes (Fig. 3F). This is similar to the rearrangement of nuclei to align in the acinus wall in response to HGF (Fig. 1C). These suggest that clustering and activation of peripheral β1-integrins in cell aggregates may induce localized signalling at the basolateral-ECM interface to prompt acinus formation.

To investigate this further we examined a common signalling effector of β1-integrins; the kinase c-Src [13]. In 2D, HGF stimulation induced activation of c-Src, which could be blocked by either a c-Src inhibitor or by blocking β1-integrins (Fig. S1B, C). In 3D, HGF induced a somewhat delayed activation of c-Src, concomitant with an increase in total c-Src levels (Fig. 3G). We noted polarization of activated c-

Src (pY416-c-Src; p-c-Src) similar to β1-integrin in response to HGF, moving from general cortical localization to exclusively basolateral membranes (Fig. 3F). c-Src was required for HGF induced morphogenesis, as chemical inhibition or depletion of c-Src with either of two shRNAs resulted in a robust inhibition of acinus formation in response to HGF (Fig. 3H-J). c-Src is thus a major target of HGF signalling in acinar morphogenesis. -

3.4 Inhibition of the RhoA-ROCK1 signalling pathway is required for acinar polarization.

In MDCK cysts, β1-integrin signalling inhibits apical domain formation at the ECM-abutting cyst periphery by promoting peripheral phosphorylation of the RhoA-specific inactivator p190A RhoGAP (hereforth referred to as p190A) [9]. In Calu-3 in 3D, HGF-c-Src signalling regulated p190A re-localization rather than controlling p190A phosphorylation (Fig. 4A, B).

In control aggregates, p190A localized to cell-cell contacts, but was absent from ECM-abutting membranes. HGF induced p190A re-localization exclusively to the basolateral domain (Fig. 4A), mirroring that observed for β1-integrin and pY416-c-Src (Fig. 3). P190A was required for HGF-induced acinus formation, as p190A depletion resulted in highly disorganized aggregates displaying inverted polarity despite HGF stimulation (Fig. 4C-E). This could be rescued by inhibition of Rho Kinase (ROCK1/2) (Fig. 4E), confirming that p190A is acting as an inhibitor of the Rho-ROCK pathway to control polarity orientation.

Our data reveal that the ROCK signalling pathway may be sufficient to promote acinus formation in 3D Calu-3. Depletion of RhoA and ROCK1, but not ROCK2, was sufficient to induce acinus formation, abolishing the requirement for HGF (Fig. 4G-L). These data suggest that HGF activates a c-Src- and β1-integrin-dependent pathway that converges upon a RhoA-ROCK1 inhibitory module to control acinus formation.

Given that FCM, HGF, and ROCK inhibition can all induce acinus formation, we examined signalling pathways that may overlap to control polarity reorientation (Fig S1E-F). FCM, activated EGFR mutants, and to a lesser extent HGF, robustly

activated ERK (Fig 2E, Fig. S1E-F). Inhibition of ERK in HGF-treated cells did not block morphological rearrangement into a contiguous, spherical monolayer, rather causing a reduction of acinus size and the lack of a lumen (Fig. S1E-G). This is highly similar to EGFR inhibition (Fig. S2D, F), suggesting that activation of ERK may be a major contribution of EGFR to Calu-3 morphogenesis. Discordant activation magnitudes between FCM and HGF for p-p38MAPK, p-MSK1/2, p-RSK1-3, and p-CREB were observed, suggesting that these may be related to off-target effects of FCM (Fig. S1E). In contrast, activation amplitude of p-Akt1-3 was consistent between FCM and HGF, suggesting that a common level of PI3-kinase pathway activation between these two conditions may regulate acinus formation. The morphogenetic effect of FCM could be completely abolished by inhibition of PI3-Kinase and mTOR pathway inhibition (Fig. S1H). Akt inhibition significantly, though only partially, attenuated acinus formation, suggesting that PI3K controls acinus apical polarity through Akt-dependent and -independent mechanisms (Fig. S1H). Surprisingly, ROCK inhibition failed to induce activation of any of the aforementioned pathways (Fig. S1E), suggesting that ROCK is downstream to these pathways in acinus formation.

These data reveal an HGF:c-Met-dependent activation of integrin-based adhesion to regulate polarity through c-Src:p190A-dependent inhibition of RhoA-ROCK1 signalling. As a similar pathway exists in MDCK cysts [6], and the correct orientation of polarity can be ‘rescued’ in organoid cultures from patients displaying inverted polarity [14], our data suggest a conserved role for p190A, RhoA, and ROCK1 in controlling epithelial polarity orientation.

4. Conclusions

In this study, we set out to examine the mechanisms of apical-basal polarity orientation pathways in 3D culture. We identified a highly similar pathway of polarity orientation in Calu-3 acini as MDCK cysts culture, indicating a conservation of polarity mechanisms [6]. In both systems, β1-integrin is required to localize a kinase to basolateral membranes to phosphorylate p190A RhoGAP at a site, which brings it into a complex with β1-integrins. c-Src and FAK are central to this in both MDCK and Calu-3 acini (unpublished observations). This sets up a zone of inhibition against the

RhoA GTPase at the ECM-abutting membrane of cells, resulting in the inhibition of RhoA and its downstream kinase ROCK1. This collectively allows the reorientation of apical-basal polarity to form a lumen.

Most studies examining epithelial polarity almost exclusively utilize isolated epithelial cells. Even in such systems the regulation of polarity orientation is only recently becoming clear, and how non-epithelial cells may influence epithelial polarity is largely unknown. In Calu-3 cells in 3D, though the polarity-regulating pathway exists, it is not localized to the correct domain – the basolateral domain - at steady state. This requires activation by HGF/c-Met signalling, which can occur upon paracrine signalling by fibroblast-derived HGF. It will thus be important in future studies to examine co-culture of epithelia with other cell types, to determine how these influence cell polarity.

The RhoA-ROCK1 signalling pathway is a major regulator of polarity orientation [3, 4, 6, 7], and our current and previous results indicate that it must be under strict spatiotemporal control to allow for the correct orientation of apical-basal polarization. Given the largely overlapping targets of ROCK1 and ROCK2 it is surprising that only ROCK1 inhibition is responsible for polarity reorientation. In the MDCK system, the Podocalyxin-NHERF1-Ezrin complex is a target of RhoA-ROCK1 pathway in polarity reorientation [6], but we were unable to detect Podocalyxin expression in Calu-3 (unpublished observations), suggesting alternate targets of ROCK1 must regulate polarity in these cells. It will be important to determine in future work the targets of ROCK1 in controlling polarity.

That HGF can induce acinar polarization of Calu-3 lung adenocarcinoma cells is striking, as HGF has been identified as a key factor secreted by lung stroma that promotes the survival of lung cancer cells *in vivo* [15, 16]. EGFR in our system regulated growth and temporary downregulation was required for lumen clearance. Polarization thus requires both growth regulation and polarity regulation systems to be co-ordinated. Acinar polarization has been shown in other systems to promote resistance to cell death-inducing treatments [17]. What the functional consequence of promoting acinus formation is for treatment for cancer therapies is unknown, but it

is tempting to speculate that this may promote survival of lung cancer cells, though this possibility awaits future formal testing.

In summary, our data indicate conserved ability of a β1-integrin-p190A RhoGAP module in controlling RhoA-ROCK1 signalling for the correct orientation of cell polarity. We now demonstrate that whether this pathway is active in cancer cells may depend on the cellular context and may be controlled in a non-cell autonomous fashion. An unmet need is to understand how to kill residual tumour cells that are resistant to inhibition of cell growth pathways. Our work provides a hint that targeting both proliferation and polarity pathways might be an unrealised, yet effective route to kill residual, resistant cancer cells.

Conflict of interest

The authors declare no conflicts of interest.

Acknowledgements

We thank the many investigators that shared reagents. Supported by NIH grants R01DK074398, R01DK091530 and 2P50 GM081879 (KM), and K99CA163535 (DB).

Author contributions

AD performed the experiments. AD and DB designed experiments and analysed data. DB and ES wrote the manuscript. DB and KM supervised the study.

References

[1] D.M. Bryant, K.E. Mostov, From cells to organs: building polarized tissue., Nat Rev Mol Cell Biol 9(11) (2008) 887-901.

[2] E. Rodriguez-Boulan, I.G. Macara, Organization and execution of the epithelial polarity programme, Nat Rev Mol Cell Biol 15(4) (2014) 225-42.

[3] A.W. Overeem, D.M. Bryant, I.S.C. van, Mechanisms of apical-basal axis orientation and epithelial lumen positioning, Trends Cell Biol 25(8) (2015) 476-85.

[4] A. Roman-Fernandez, D.M. Bryant, Complex Polarity: Building Multicellular Tissues Through Apical Membrane Traffic, Traffic 17(12) (2016) 1244-1261.

[5] L.E. O'Brien, M.M. Zegers, K.E. Mostov, Opinion: Building epithelial architecture: insights from three-dimensional culture models, Nat Rev Mol Cell Biol 3(7) (2002) 531-7.

[6] D.M. Bryant, J. Roignot, A. Datta, A.W. Overeem, M. Kim, W. Yu, X. Peng, D.J. Eastburn, A.J. Ewald, Z. Werb, K.E. Mostov, A molecular switch for the orientation of epithelial cell polarization, Developmental cell 31(2) (2014) 171-87.

[7] W. Yu, A.M. Shewan, P. Brakeman, D.J. Eastburn, A. Datta, D.M. Bryant, Q.W. Fan, W.A. Weiss, M.M. Zegers, K.E. Mostov, Involvement of RhoA, ROCK I and myosin II in inverted orientation of epithelial polarity., EMBO Rep 9(9) (2008) 923-9.

[8] A.L. Pollack, A.I. Barth, Y. Altschuler, W.J. Nelson, K.E. Mostov, Dynamics of beta-catenin interactions with APC protein regulate epithelial tubulogenesis, J Cell Biol 137(7) (1997) 1651-62.

[9] D.M. Bryant, A. Datta, A.E. Rodríguez-Fraticelli, J. Peränen, F. Martín-Belmonte, K.E. Mostov, A molecular network for de novo generation of the apical surface and lumen., Nat Cell Biol 12(11) (2010) 1035-45.

[10] D. Bryant, K. Mostov, Development: inflationary pressures., Nature 449(7162) (2007) 549-50.

[11] Y. Zhu, A. Chidekel, T.H. Shaffer, Cultured human airway epithelial cells (calu-3): a model of human respiratory function, structure, and inflammatory responses, Crit Care Res Pract 2010 (2010).

[12] R. Montesano, K. Matsumoto, T. Nakamura, L. Orci, Identification of a fibroblast-derived epithelial morphogen as hepatocyte growth factor, Cell 67(5) (1991) 901-8.

[13] S.K. Mitra, D.D. Schlaepfer, Integrin-regulated FAK-Src signaling in normal and cancer cells, Curr Opin Cell Biol 18(5) (2006) 516-23.

[14] A.E. Bigorgne, H.F. Farin, R. Lemoine, N. Mahlaoui, N. Lambert, M. Gil, A. Schulz, P. Philippet, P. Schlesser, T.G. Abrahamsen, K. Oymar, E.G. Davies, C.L. Ellingsen, E. Leteurtre, B. Moreau-Massart, D. Berrebi, C. Bole-Feysot, P. Nischke, N. Brousse, A. Fischer, H. Clevers, G. de Saint Basile, TTC7A mutations disrupt intestinal epithelial apicobasal polarity, J Clin Invest 124(1) (2014) 328-37.

[15] K. Matsumoto, M. Umitsu, D.M. De Silva, A. Roy, D.P. Bottaro, Hepatocyte growth factor/MET in cancer progression and biomarker discovery, Cancer Sci 108(3) (2017) 296-307.

[16] R. Straussman, T. Morikawa, K. Shee, M. Barzily-Rokni, Z.R. Qian, J. Du, A. Davis, M.M. Mongare, J. Gould, D.T. Frederick, Z.A. Cooper, P.B. Chapman, D.B. Solit, A. Ribas, R.S. Lo, K.T. Flaherty, S. Ogino, J.A. Wargo, T.R. Golub, Tumour micro-environment elicits innate resistance to RAF inhibitors through HGF secretion, Nature 487(7408) (2012) 500-4.

[17] T. Muranen, L.M. Selfors, D.T. Worster, M.P. Iwanicki, L. Song, F.C. Morales, S. Gao, G.B. Mills, J.S. Brugge, Inhibition of PI3K/mTOR leads to adaptive resistance in matrix-attached cancer cells, Cancer Cell 21(2) (2012) 227-39.

Figure Legends

Figure 1: Fibroblast Conditioned Medium (FCM) induces the formation of polarized Calu-3 acini.

(A) Schematic showing the experimental procedure for developing Calu-3 acini in 3D with key modifiers added or removed between days 4-9.

(B) Calu-3 cells were cultured on a layer of Matrigel in standard growth media containing 2% Matrigel. After 4 days the media on the resultant aggregates was either replenished or replaced with FCM. Acini were fixed on day 9, stained with F-actin and imaged using a confocal microscope.

(C) Acini were fixed and stained at different time points post addition of FCM at day 4, with anti-Ki-67 (magenta), anti-Cleaved Caspase-3 (green) and F-actin (black) antibodies. Arrows indicate the localization of Ki-67. Magnified images are also shown (lower panels).

(D) Untreated or FCM treated acini were fixed and stained with Hoechst (blue) and either Phalloidin, anti-JAM-A, anti-β-catenin, anti-Muc1 anti-NHERF-1, anti-Ezrin or anti-GM130 antibodies (all green). Arrows indicate the localization of Muc-1. Insets show magnified images.

All scale bars, 50 μm.

Figure 2: HGF and EGF stimulate Calu-3 acinus formation, regulating polarity and proliferation respectively.

(A) Calu-3 aggregates were treated on day 4 with FCM, HGF (10 ng/ml), FCM + HGF mAb (0.1 μg/mL) or FCM + SU11274 (10 μM) and fixed on day 9. Graph shows the number of acini with a single central lumen. Results are presented as mean percentage +/- s.d. and significance is ***$p \leq 0.0001$ (n=3).

(B) Aggregates/acini formed in the absence or presence of HGF were fixed and stained with either anti-Cleaved Caspase 3 (green in upper panels) or anti-Cleaved Caspase 8 antibodies (green in lower panels) and F-actin (red) and Hoechst (blue).

(C) Aggregates/acini formed in the absence or presence of exogenous EGF (10 ng/ml) were fixed and stained with Muc1 antibody (white in upper panels) and Hoechst (magenta in upper panels). Maximum intensity projection (MIP) of Muc1 staining is also shown (lower panels). Arrows indicate apical localization of Muc1.

(D) EGFR signalling was inhibited using Iressa (1 μM) in the presence of HGF and samples stained with F-actin (white) and Hoechst (magenta).

(E) Parental or EGFR mutant-expressing (L858R, Δ3 A750P) cells were harvested for Western blotting. Immunoblotting was performed using anti-EGFR, anti-pErk1/2 and anti-GAPDH antibodies.

(F) Aggregates expressing either EGFR-L858R or EGFR-Δ3 A750P and stimulated with HGF and either with or without Iressa (1 μM), were fixed and stained with anti-cleaved caspase-3 antibody (green), F-actin (red) and Hoechst (blue).

All scale bars, 50 μm.

Figure 3: c-Src is a major target of HGF signalling in acinar morphogenesis.

(A) Phase images of Calu-3 cells grown on plastic in presence or absence of HGF.

(B) Graph shows the percentage of Calu-3 cells adhering to plastic after treatment with HGF and either AIIB2, a β1 integrin blocking antibody (1:200), or TS2/16, a β1 integrin activating antibody (1:100), all normalized to non-treated control cells (NT).

(C) Aggregates treated with TS2/16 or with HGF and AIIB2, were fixed and stained with F-actin (red) and Hoechst (blue).

(D) Graph shows the percentage of acini with a single central lumen upon treatment with either control antibody (Co. mAb), HGF, AIIB2 or TS2/16.

(E) Surface expression of β1 integrin in control and HGF treated Calu-3 cells in 2D was examined by FACS analysis.

(F) Untreated aggregates or HGF treated acini were fixed and stained with anti-β1 integrin (green in upper panels) or anti-pY416-c-Src (green in lower panels) antibodies and F-actin (red) and Hoechst (blue). A magnified image of anti-β1 integrin (upper middle panels) and anti-pY416-c-Src (lower middle panels) in untreated and HGF treated samples is also shown (a and b respectively).

(G) Aggregates were stimulated with HGF and harvested at various time-points. Immunoblotting was performed using anti-pY416-c-Src, anti-c-Src and anti-GAPDH antibodies.

(H) c-Src protein expression was reduced in Calu-3 cells using either of 2 different shRNAs and knockdown confirmed by immunoblotting with anti-c-Src and anti-GAPDH antibodies.

(I) Graph shows the percentage of acini with a single central lumen after c-Src knockdown and HGF stimulation.

(J) Aggregates expressing Scramble or c-Src shRNA were stimulated with HGF, fixed and stained with anti-Muc1 antibody (green), F-actin (red) and Hoechst (blue). Arrows indicate localization of Muc1 at membranes. Insets show magnified images of Muc1 localization (green).

All graphs are presented as mean percentage +/- s.d. and significance is *p≤0.05 and ***p≤0.0001 (n= 3). All scale bars, 50 µm.

Figure 4: A RhoA-ROCK1 inhibitory module downstream of c-Src and β1 integrin controls acinus formation.

(A) Aggregates were treated with HGF, fixed and stained with pY1105-p190A RhoGAP antibody (black) and Hoechst (magenta). Magnified images of pY1105-p190A RhoGAP localization in untreated and HGF stimulated samples (middle panels, a and b respectively) are shown. Red arrows indicate lack of pY1105-p190A RhoGAP while green arrows show its localization to membranes.

(B) Aggregates treated with HGF and the c-Src inhibitor PP2 (5 µM), were harvested and immunoblotted with anti-pY1105-p190A RhoGAP and anti-GAPDH antibodies.

(C) P190A RhoGAP expression was reduced in Calu-3 cells using either of 2 different shRNAs and knockdown confirmed by immunoblotting with anti-p190A RhoGAP, anti-pY1105-p190A RhoGAP and anti-GAPDH antibodies.

(D) Calu-3 aggregates expressing Scramble or p190A RhoGAP shRNA were stimulated with HGF then fixed and stained with anti-Muc1 antibody (green), F-actin (red) and Hoechst (blue). Arrows indicate localization of Muc1 at membranes. Insets show magnified images of Muc1 localization (green).

(E) Graph shows the percentage of acini with a single central lumen after treatment with HGF and Rho Kinase (ROCK1/2) inhibitor, Y-27632 (10 µM).

(F) RhoA, ROCK1 and ROCK2 were depleted in Calu3 cells using specific shRNAs and samples stained with anti-Muc1 antibody (green), F-actin (red) and Hoechst (blue). Arrows indicate localization of Muc1 at membranes.

(G) Knockdown with either of 2 different shRNAs was confirmed by immunoblotting with anti-RhoA (H) anti-ROCK1 and (I) anti-ROCK2 antibodies. GAPDH antibody was used as a control.

(J) Graphs show the percentage of acini with a single central lumen after knockdown of RhoA or (K) ROCK1 and ROCK2.

All graphs are presented as mean percentage +/- s.d. and significance is *p≤0.05, **p≤0.001 and ***p≤0.0001 (n= 3). All scale bars, 50 µm.

Supplementary Figure 1: Signalling pathways regulating acinar morphogenesis.

(A) Calu-3 aggregates were stimulated with HGF for 120 hours and samples taken at different time points. Immunoblotting was performed using anti-pY416-c-Src, anti-c-Src, anti-pY845 EGFR, anti-EGFR and anti-GAPDH antibodies.

(B) Aggregates were stimulated with HGF and either PP2 (5 µM), AIIB2 (1:200) or TS2/16 (1:100). Immunoblotting was carried out using anti-pY416-c-Src anti-GAPDH antibodies.

(C) HGF stimulated aggregates were treated with PP2 and stained with anti-pY416-c-Src (green) and Hoechst (blue). Insets show magnified images of pY416-c-Src (middle panels) in untreated (a) or HGF treated (b) samples.

(D) Graph shows the percentage of acini with a single central lumen after treatment with HGF and Y-27632 (10 µM).

(E) Aggregates were stimulated with FCM, HGF or Y-27632 and a kinase array carried out. Graph shows the fold change in activation amplitude of pp-Erk1/2, p-p38MAPK, p-MSK1/2, p-RSK1-3, p-Akt1-3, p-CREB and p-β-catenin.

(F) Immunoblotting was performed on FCM treated aggregates using anti-pp-ERK1/2 and anti-GAPDH antibodies.

(G) HGF stimulated aggregates were also treated with U016, a MEK inhibitor (10 µM), and then fixed and stained with anti-Muc1 antibody (black), F-actin (magenta) and Hoechst (green). Insets show magnified images of Muc1 localization (black).

(H) Graph shows the percentage of acini with a single central lumen after treatment with LY-294002 (10 µM), Akt Inhibitor-II (10 µM) or rapamycin (20 nM) after stimulation with FCM.

All graphs are presented as mean percentage +/- s.d. and significance is *p≤0.05, **p≤0.001 and ***p≤0.0001 (n= 3). All scale bars, 50 µm.

Figure 1

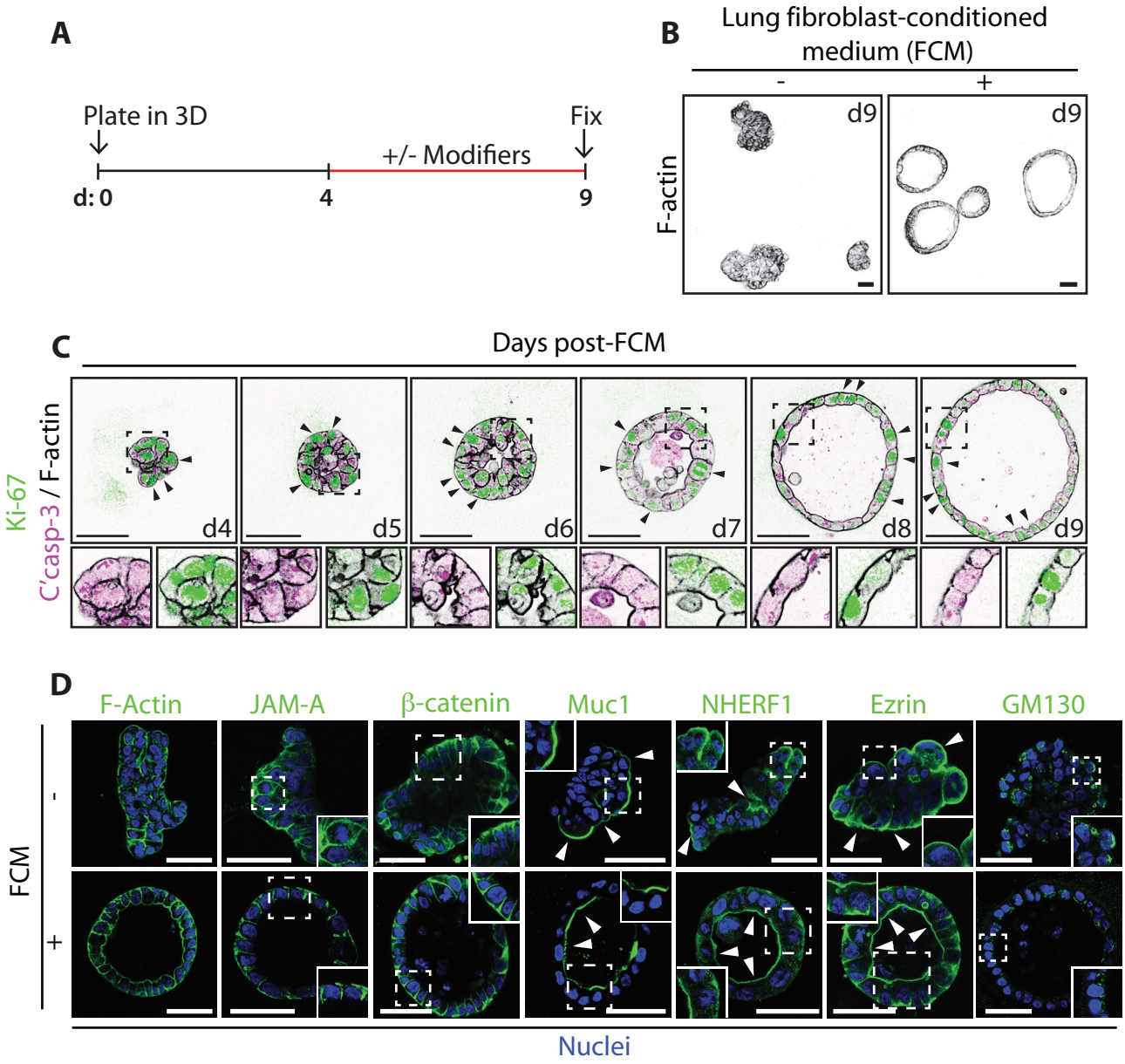
A
Plate in 3D
Fix
+/- Modifiers
d: 0
4
9
B
Lung fibroblast-conditioned medium (FCM)
-
+
F-actin
d9
d9
C
Days post-FCM
Ki-67
C'casp-3 / F-actin
d4
d5
d6
d7
d8
d9
D
F-Actin
JAM-A
β-catenin
Muc1
NHERF1
Ezrin
GM130
FCM
-
+
Nuclei

Figure 2

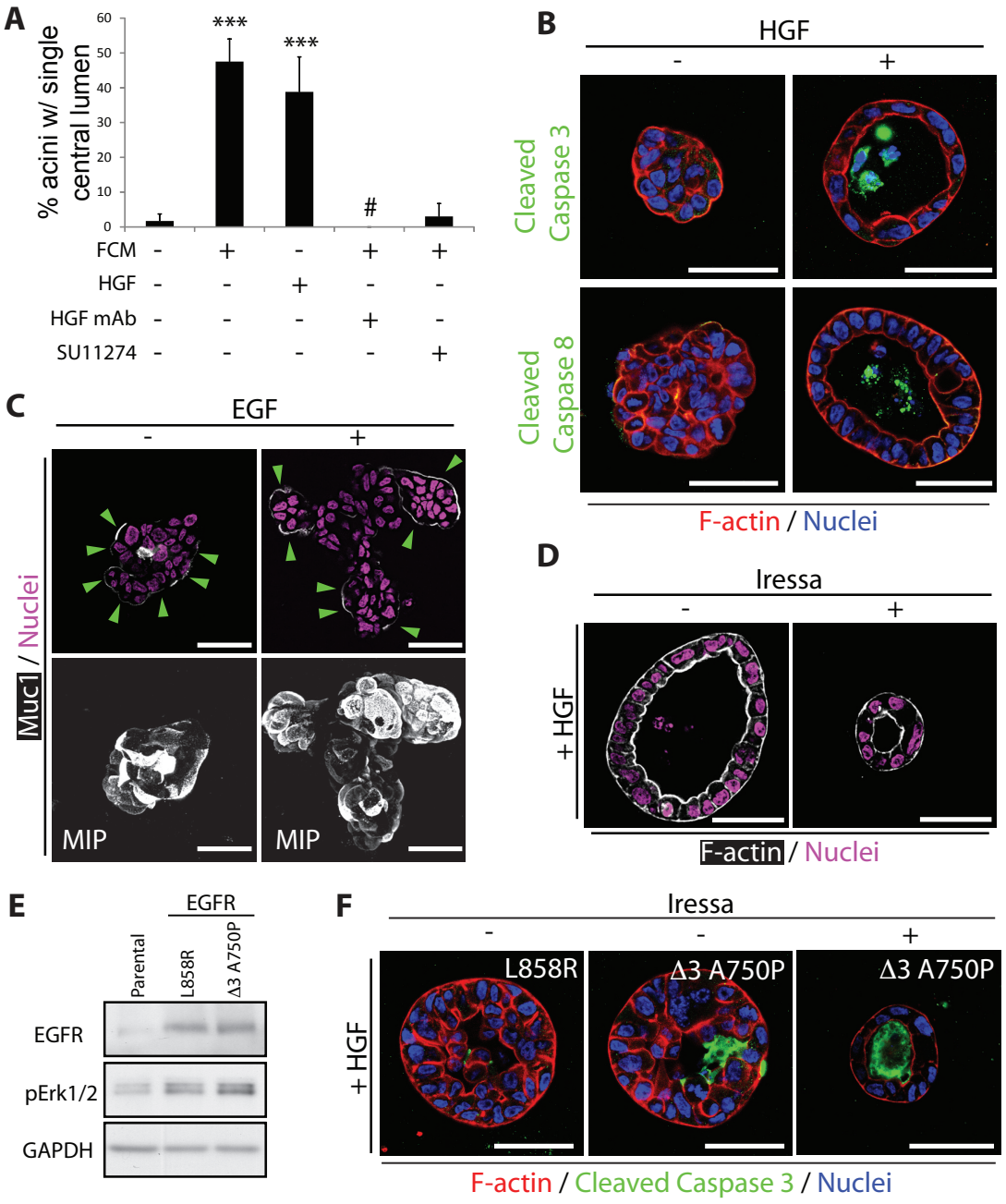
A
% acini w/ single central lumen
60
50
40
30
20
10
0
***
***
#
FCM - + - + +
HGF - - + - -
HGF mAb - - - + -
SU11274 - - - - +
B
HGF
-
+
Cleaved Caspase 3
Cleaved Caspase 8
F-actin / Nuclei
C
EGF
-
+
Muc1 / Nuclei
MIP
MIP
D
Iressa
-
+
+ HGF
F-actin / Nuclei
E
EGFR
Parental
L858R
Δ3 A750P
EGFR
pErk1/2
GAPDH
F
Iressa
-
-
+
+ HGF
L858R
Δ3 A750P
Δ3 A750P
F-actin / Cleaved Caspase 3 / Nuclei

Figure 3

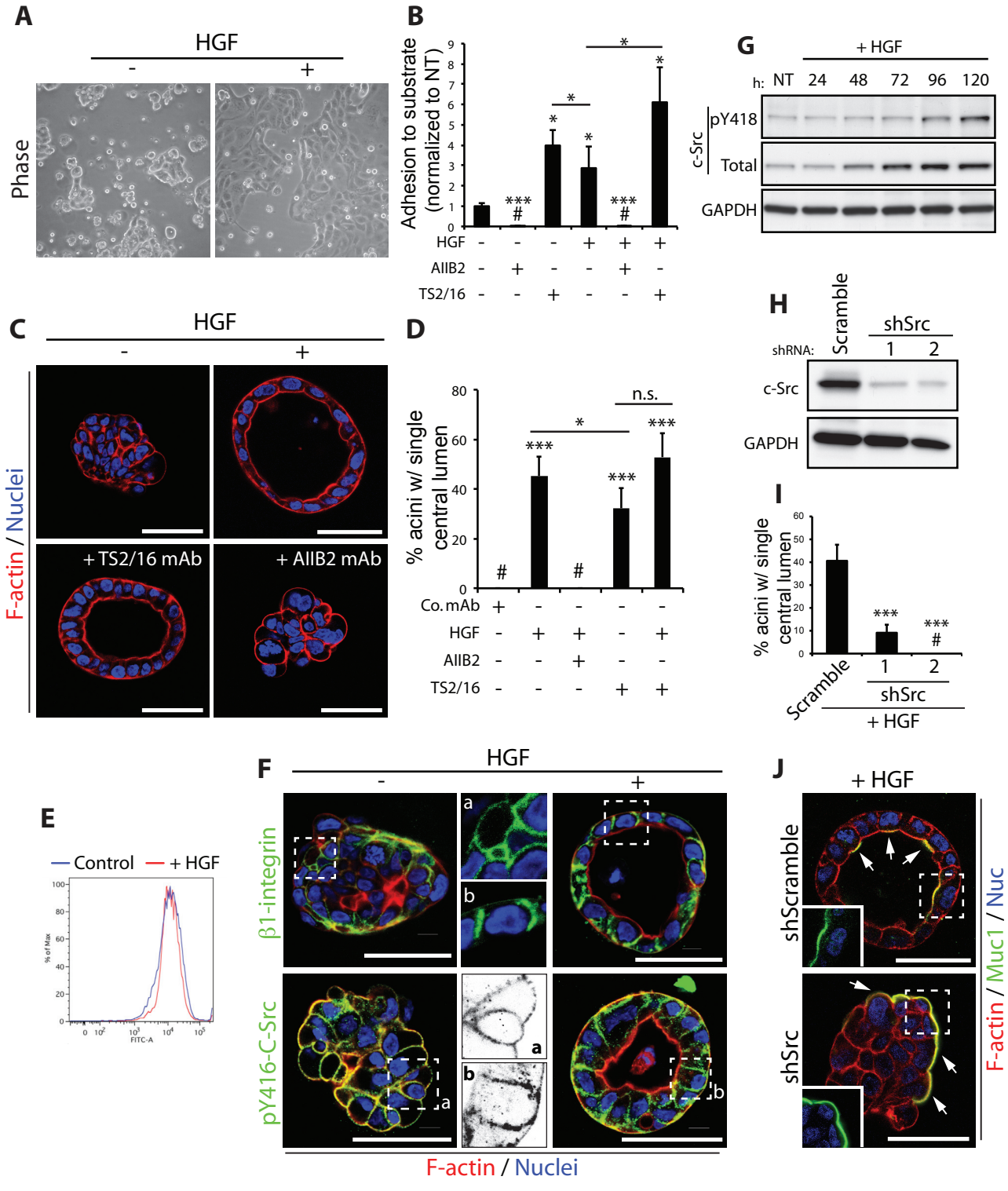
Figure 3
A
HGF
-
+
Phase
B
Adhesion to substrate (normalized to NT)
HGF
AIIB2
TS2/16
G
+ HGF
h: NT 24 48 72 96 120
c-Src
pY418
Total
GAPDH
C
HGF
F-actin / Nuclei
+ TS2/16 mAb
+ AIIB2 mAb
D
% acini w/ single central lumen
n.s.
Co. mAb
HGF
AIIB2
TS2/16
H
Scramble
shSrc
shRNA:
1
2
c-Src
GAPDH
I
% acini w/ single central lumen
Scramble
shSrc
+ HGF
E
Control
+ HGF
% of Max
FITC-A
F
HGF
β1-integrin
pY416-C-Src
F-actin / Nuclei
J
+ HGF
shScramble
shSrc
F-actin / Muc1 / Nuc

Figure 4

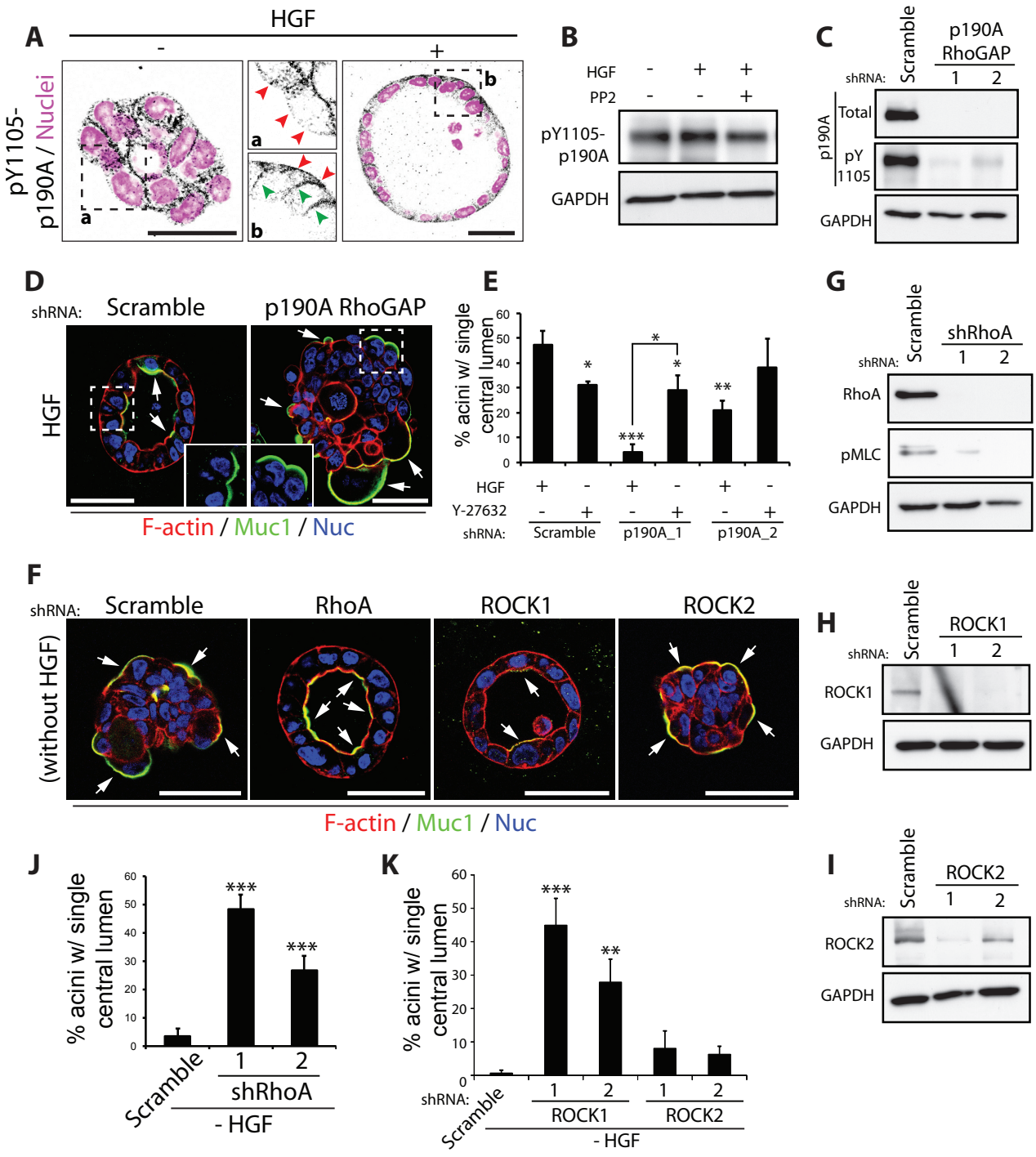
A
HGF
-
+
pY1105-p190A / Nuclei
a
b
B
HGF
PP2
pY1105-p190A
GAPDH
C
Scramble
p190A RhoGAP
shRNA:
1
2
p190A
Total
pY 1105
GAPDH
D
shRNA:
Scramble
p190A RhoGAP
HGF
F-actin / Muc1 / Nuc
E
% acini w/ single central lumen
HGF
Y-27632
shRNA:
Scramble
p190A_1
p190A_2
G
Scramble
shRhoA
shRNA:
1
2
RhoA
pMLC
GAPDH
F
shRNA:
Scramble
RhoA
ROCK1
ROCK2
(without HGF)
F-actin / Muc1 / Nuc
H
Scramble
ROCK1
shRNA:
1
2
ROCK1
GAPDH
I
Scramble
ROCK2
shRNA:
1
2
ROCK2
GAPDH
J
% acini w/ single central lumen
Scramble
shRhoA
1
2
- HGF
K
% acini w/ single central lumen
shRNA:
Scramble
ROCK1
ROCK2
1
2
- HGF

Figure S1

Supplementary Figure 1